Biochimica et Biophysica Acta 1850 (2015) 750–758

Contents lists available at ScienceDirect

Biochimica et Biophysica Acta

journal homepage: www.elsevier.com/locate/bbagen

Andrographolide decreased VEGFD expression in hepatoma cancer cells by inducing ubiquitin/proteasome-mediated cFos protein degradation

Lili Ji [a,b,*], Zhiyong Zheng [a], Liang Shi [a], Yinjie Huang [a], Bin Lu [a], Zhengtao Wang [a,b,*]

[a] Shanghai Key Laboratory of Complex Prescription and The MOE Key Laboratory for Standardization of Chinese Medicines, Institute of Chinese Materia Medica, Shanghai University of Traditional Chinese Medicine, Shanghai 201203, China

[b] The SATCM Key Laboratory for New Resources and Quality Evaluation of Chinese Medicines, Institute of Chinese Materia Medica, Shanghai University of Traditional Chinese Medicine, Shanghai 201203, China

ARTICLE INFO

Article history:
Received 21 September 2014
Received in revised form 24 December 2014
Accepted 7 January 2015
Available online 14 January 2015

Keywords:
Andrographolide
Hepatoma cancer
cFos
VEGFD
Protein degradation

ABSTRACT

Background: Andrographolide (Andro) is reported to inhibit hepatoma tumor growth in our previous studies. This study aims to further search the critical signals involved in such Andro-induced inhibition.

Methods: The anti-tumor effect of Andro was evaluated *in vivo*. Cancer PathwayFinder RT^2 Profiler™ PCR array was used to find the altered genes. Real-time PCR was used to detect the mRNA expression. Protein expression was detected by Western-blot analysis, enzyme-linked immunosorbent assay (ELISA) and immunohistochemical staining. Activator protein-1 (AP-1) transcriptional activity was detected by luciferase reporter assay.

Results: Andro (10 mg/kg) inhibited hepatoma tumor growth *in vivo*. The expression of four genes decreased in Andro-treated tumor tissues. Among which, vascular endothelial growth factor (VEGFD) was the highest decreased gene. The decreased VEGFD expression was further confirmed by real-time PCR and immunohistochemical staining assay. Andro decreased VEGFD mRNA and protein expression in hepatoma Hep3B and HepG2 cells. Andro also decreased VEGFD amount in Hep3B cell supernatant. Andro decreased cFos protein expression and its translocation into nucleus, and also reduced AP-1 luciferase activity. Further results showed that Andro induced polyubiquitination of cFos. Proteasome inhibitor MG132 reversed the decreased expression of cFos protein, and the decreased mRNA and protein expression of VEGFD. SP600125, an inhibitor of c-Jun N-terminal kinase (JNK), reversed the decreased expression of cFos and VEGFD induced by Andro.

Conclusions: Andro decreased VEGFD expression in hepatoma cancer cells via inducing c-fos protein degradation, which will contribute to its anti-cancer activity, and JNK plays some roles in regulating this process.

1. Introduction

Andrographolide (Andro), a natural diterpenoid lactone, is the main compound isolated from traditional medicinal herb *Andrographis paniculata* Nees (Acanthaceae) [1]. Andro is reported to have various biological activities such as anti-inflammatory, antibacterial, antivirus, and anti-cancer effects [1,2]. The anti-cancer effect of Andro attracts more and more attention in the recent years, and Andro was reported to have potential therapeutic function for liver cancer, non-small-cell lung cancer, breast cancer, pancreatic cancer, etc. [3–7]. Our previous studies have already demonstrated that Andro inhibited hepatoma tumor growth *in vivo* and *in vitro*. In addition, regulating cellular JNK activation and glutathione homeostasis, and inhibiting VEGF-mediated angiogenesis contribute greatly to Andro-induced inhibition on hepatoma tumor growth [8–11]. However, whether there are other signals critically involved in the inhibition of Andro on hepatoma tumor growth is not very clear.

Tumor angiogenesis provides oxygen and nutrients for the growth, invasiveness and metastasis of tumor; and blocking angiogenesis has been an effective strategy for the cancer therapy in the recent years [12]. Our previous study has already shown that Andro can inhibit angiogenesis via inhibiting the activation of VEGF/VEGFR2-MAPK signaling cascade [8]. Vascular endothelial growth factor (VEGFD), also named cFos induced growth factor (FIGF), is a member of VEGF family [13]. Except the major pro-angiogenic factor VEGF, VEGFD is also reported to induce angiogenesis *in vivo* and *in vitro* through binding with VEGFR2 [14,15]. In addition, VEGFD can bind with VEGFR3, which is expressed in lymphatic endothelial cells, and induce the formation of new lymphatic vessels, which is called lymphangiogenesis [15,16]. Recently, lymphangiogenesis is reported to be related with the lymph node metastasis of tumor, which is commonly occurred in cancer, and

Abbreviations: Andro, Andrographolide; VEGFD, Vascular endothelial growth factor D; ELISA, Enzyme-linked immunosorbent assay; AP-1, Activator protein-1; JNK, c-Jun N-terminal kinase; MAPK, Mitogen-activated protein kinase; VEGF, Vascular endothelial growth factor; MMP2, Matrix metallopeptidase 2; MTA1, Metastasis associated 1; EGFR, Epidermal growth factor receptor; HCC, Hepatocellular carcinoma

* Corresponding authors at: Institute of Chinese Materia Medica, Shanghai University of Traditional Chinese Medicine, 1200 Cailun Road, Shanghai 201203, China. Tel.: +86 21 51322517; fax: +86 21 51322505.

E-mail addresses: lichenyue1307@126.com (L. Ji), ztwang@shutcm.edu.cn (Z. Wang).

http://dx.doi.org/10.1016/j.bbagen.2015.01.005
0304-4165/

has been a potent target for cancer therapy [17–20]. In the present study, the results of Cancer PathwayFinder RT^2 Profiler™ PCR array first showed that the expression of VEGFD was highly decreased in tumor tissues after Andro treatment. Further study was conducted to observe the decreased expression of VEGFD induced by Andro in hepatoma cells and the engaged mechanisms.

2. Materials and methods

2.1. Chemical compounds and reagents

Andrographolide (Andro) was purchased from Nanjing TCM Institute of Chinese Materia Medica (Nanjing, China). The chemical structure of Andro is shown in Fig. 1A. The purity of the compound was over 98.5% as determined by high pressure liquid chromatography (HPLC) analysis. RT^2 Profiler™ PCR array was purchased from Qiagen (Hilden, German). Trizol reagent was purchased from Life Technology (Carlsbad, CA). PrimeScript® RT Master Mix and SYBR® Premix Ex Taq™ were purchased from Takara (Shiga, Japan). The DAKO EnVision™ detection system was purchased from DAKO Corporation (Carpinteria, CA). Whole cell extraction kit, RIPA lysis buffer, enhanced chemiluminescence kit, and Catch and Release® reversible immunoprecipitation system were all obtained from Millipore (Darmstadt, Germany). NE-PER® nuclear and cytoplasmic extraction reagents and Pierce® BCA Protein Assay Kit were purchased from Thermo Scientific (Bremen, Germany). VEGFD antibody and enzyme-linked immunosorbent assay (ELISA) kit for VEGFD were purchased from R&D (Minneapolis, MN). Duan-Glo® Luciferase Assay System and pGL4.44 (*luc*2P/AP1 RE/Hygro) vector were purchased from Promega (Madison, WI). Histone H3, Ubiquitin, cFos, and β-actin antibodies were purchased from Cell Signaling Technology (Danvers, MA). cFos for immunoprecipitation assay was purchased from Santa Cruz (Santa Cruz, CA). Peroxidase-conjugated goat anti-Rabbit IgG (H + L) and peroxidase-conjugated goat anti-Mouse IgG (H + L) were purchased from Jackson ImmunoResearch (West Grove, PA). SP600125 was purchased from Alexis Biochemicals (San Diego, CA). Other reagents unless indicated were purchased from Sigma Chemical Co. (St. Louis, MO).

2.2. Cell lines and culture

Hepatoma-derived Hep3B and HepG2 cell lines were obtained from the American Type Culture Collection (Manassas, VA). Cells were cultured in MEM media supplemented with 10% [v/v] heat-inactivated fetal bovine serum, 2 mM glutamine, 100 U/ml penicillin and 100 mg/ml streptomycin.

2.3. In vivo tumor xenograft assay

Specific pathogen-free nude male mice (6–8 weeks of age) were obtained from Shanghai Experimental Animal Center of Chinese Academy of Sciences (Shanghai, China). All animal experiments were performed according to the protocol approved by the Experimental Animal Ethical Committee of Shanghai University of Traditional Chinese Medicine.

Mice were subcutaneously injected of Hep3B cells (1×10^6 cells per mouse) into the left front leg. After tumors had established (~30 mm^3), the mice were given daily intra-peritoneally injected of Andro at different doses (0 mg/kg, 5 mg/kg, 10 mg/kg). The tumor sizes of all mice were determined by Vernier caliper measurements and calculated as [(length × width^2)/2], and were recorded every 3 days. After 7 days, four mice of each group were sacrificed and tumors were removed for

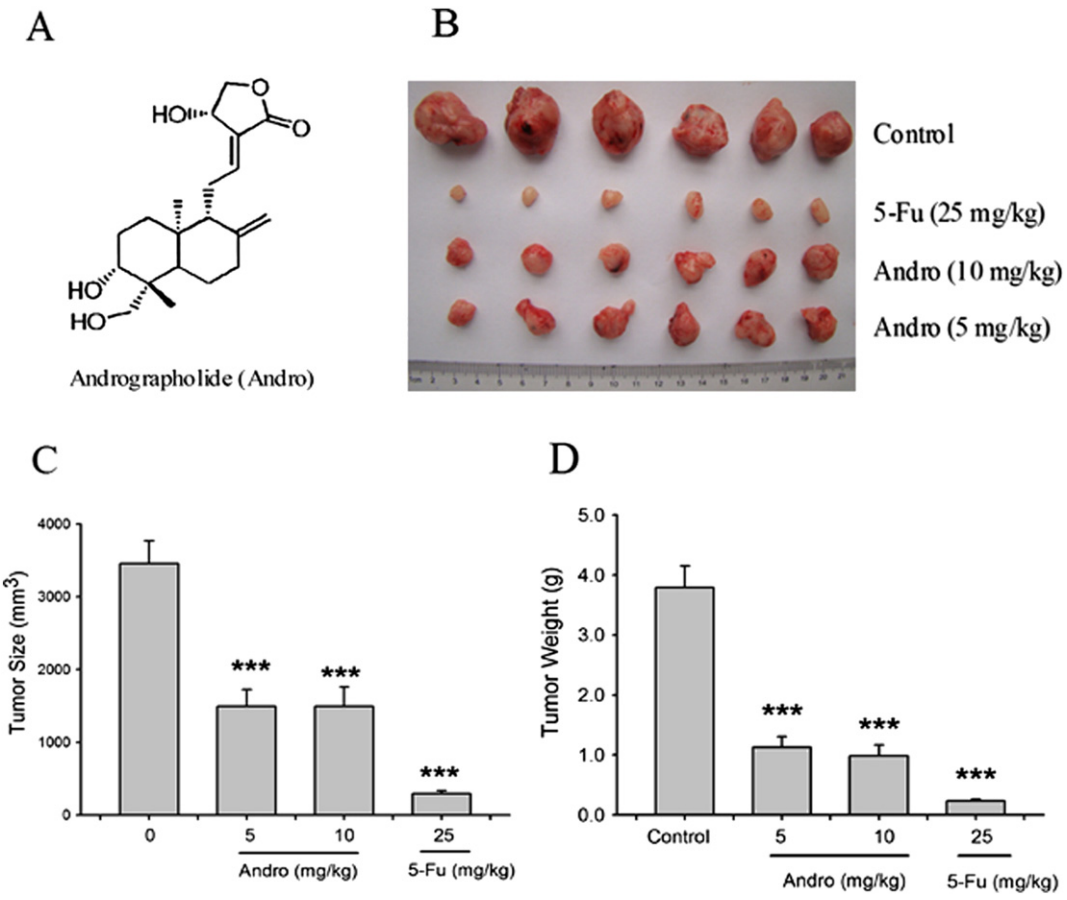

Fig. 1. Andro inhibits hepatoma tumor growth *in vivo*. **(A)** The chemical structure of andrographolide (Andro). **(B)** Tumors are removed and photographed. **(C)** Tumor sizes are recorded every 3 days and calculated as [(length × width^2)/2]. **(D)** Tumors are weighted. Data are expressed as means ± SEM (n = 6). $^{***}P < 0.001$ versus control.

immunohistochemistry. All other mice were sacrificed 16 days after Andro administration and tumors were removed, weighed and photographed.

2.4. RNA isolation and cDNA synthesis

Total RNA was isolated using Trizol reagent according to the instruction. The RNA content was determined by measuring the optical density at 260 nm, and cDNA was synthesized according to the instruction described in kits.

2.5. RT^2 Profiler™ PCR array

Cancer PathwayFinder RT^2 Profiler™ PCR array was performed for quantitative PCR with the following cycling conditions: 10 min at 95 °C, 15 s at 95 °C, and 1 min 60 °C for 40 cycles with a final 4 °C hold. Five endogenous control genes, namely, glucuronidase β, hypoxanthine guanine, heat-shock protein 90, glyceraldehyde phosphate dehidrogenase, and β-actin, were used for data normalization. Each replicate cycle threshold (Ct) was normalized to the average Ct value of five endogenous controls per plate. Results were calculated using the $2^{-\Delta\Delta Ct}$ method. Heat map was generated using the web-based program of RT^2 Profiler™ PCR array data analysis. Variations in the tumor gene expression between control and Andro-treated animals are shown as a fold of increase or decrease.

2.6. Real-time PCR analysis

Real-time PCR was performed using a SYBR green premix according to the instruction. Relative expression of target genes was normalized to Actin, analyzed by $2^{-\Delta\Delta Ct}$ method and given as ratio compared with the control. The primer sequences used in this study are shown in Supplementary Table 1.

2.7. Immunohistochemical analysis of VEGFD

Paraffin-embedded tumor sections (5 μm) were deparaffinized in xylene, and then rehydrated in a gradient of ethanol to distilled water. After quenching endogenous peroxidase activity, sections were incubated with 5% bovine serum albumin to minimize nonspecific binding. Sections were further incubated with VEGFD antibody at 4 °C overnight, and then the antigen–antibody reactions on sections were detected using DAKO EnVision™ detection kits. All sections were counterstained with hematoxylin. Images were taken under an inverted microscope (Nikon, Japan).

2.8. Protein extraction

After treatment, cellular proteins were extracted by using whole cell extraction kit according to the manufacturer's instruction. In addition, cytosolic and nuclear proteins were isolated as described in NE-PER® nuclear and cytoplasmic extraction kits.

2.9. Western-blot analysis

Proteins were separated by SDS-PAGE and blots were probed with appropriate combination of primary and horseradish peroxidase-conjugated secondary antibodies. Proteins were visualized by enhanced chemiluminescence kits. For repeated immunoblotting, membranes were stripped in 62.5 mM Tris (pH 6.7), 20% SDS and 0.1 M 2-mercaptoethanol for 30 min at 50 °C. The protein bands were quantified by the average ratios of integral optic density following normalisation to the expression of internal control β-actin, and the results were further normalized to control.

2.10. ELISA analysis

Hep3B cells were incubated with Andro (25, 50 μM) for 24 h, and VEGFD amounts in the supernatants were detected according to the manufacturer's descriptions. VEGFD concentration in the respective samples were determined on the basis of standard curves prepared using recombinant VEGFD of known concentrations.

2.11. AP-1 luciferase reporter gene assay

Hep3B cells were co-transfected with AP-1 *luc* vector (1 μg) and the control vector pGL4.50 (*luc2*/CMV/Hygro) by using Lipofectamine 3000 reagent according to the manufacturer's instructions. At 18 h after the transient transfection, cells were incubated with or without Andro (25, 50 μM) for the indicated time. Luciferase activity was measured using the Duan-Glo® Luciferase Assay System. Results were expressed as the ratio of normalized luciferase activities between Andro-treated and Andro-untreated cells.

2.12. Immunoprecipitation assay

To identify polyubiquitinated c-fos, cells were pretreated with the proteasome specific inhibitor MG132 (20 μM) for 2 h and then incubated with Andro (25, 50 μM) for another 24 h. Cells were lysed in RIPA lysis buffer and protein concentrations were determined, and then equal amounts of protein were subjected to immunoprecipitation with anti-cFos antibody as described in kits. The immunoprecipitate was separated via SDS-PAGE and the conjugates were detected with anti-ubiquitin antibody. As a control for expression of c-fos protein, Western-blot analysis was also performed with an anti-cFos antibody.

2.13. Statistical analysis

Data were expressed as means ± standard error of the mean. The significance of differences between groups was evaluated by one-way ANOVA with LSD post hoc test, and $P < 0.05$ was considered as statistically significant differences.

3. Results

3.1. Andro inhibited the tumor growth in athymic mice in vivo

First, we observed the inhibition induced by Andro on the tumor growth in athymic mice bearing hepatoma Hep3B cells. From the pictures of Fig. 1B, we can see that Andro (5 mg/kg and 10 mg/kg) obviously decreased the tumor size as compared with control group. In addition, the statistical results of daily measurement of tumor size also evidenced the inhibition of Andro (5 mg/kg and 10 mg/kg) on hepatoma tumor growth ($P < 0.001$) (Fig. 1C). Meanwhile, the results of tumor weight (Fig. 1D) showed that Andro (5 mg/kg and 10 mg/kg) decreased the tumor weight as compared with control ($P < 0.001$). The chemotherapy drug 5-fluorouracil (5-Fu) also decreased tumor weight and size in this experiment ($P < 0.001$) (Fig. 1B–D).

3.2. Andro decreased VEGFD expression in tumor tissue

To find out the critical signals involved in the inhibition on hepatoma tumor growth induced by Andro, we used Cancer PathwayFinder RT^2 Profiler™ PCR array to detect the altered gene expression. The layout of the genes in PCR array is shown in Fig. 2A, and Fig. 2B is a heat map that shows the fold regulation expression data between Andro (10 mg/kg) and the control group. As shown in Fig. 2B, some genes became green, which indicates the expression of those genes are decreased; whereas some other genes became purple red, which means the expression of those genes are increased. The differentially expressed genes over three-folds between control and Andro-treated group were listed

A

Layout	01	02	03	04	05	06	07	08	09	10	11	12
A	Akt1	Akt2	Angpt1	Apaf1	Atm	Bad	Bax	Bcl2	Bcl2l1	Birc5	Brca1	Casp8
B	Ccnd1	Ccne1	Cdc25a	Cdh1	Cdk2	Cdk4	Cdkn1a	Cdkn2a	Cflar	Chek2	Col18a1	Ctnnb1
C	E2f1	Egfr	Ets2	Fas	Fgf1	Fgfr2	Figf	Fos	Grb2	Hgf	Ifnb1	Igf1
D	Itga2	Itga3	Itga4	Itgav	Itgb1	Itgb3	Jun	Kiss1	Map2K1	Mcam	Mdm2	Met
E	Mmp2	Mmp9	Mta1	Mta2	Muc1	Myc	Ncam1	Nfkb1	Nfkbia	Nme4	Pdgfa	Pdgfb
F	Pik3r1	Plau	Plaur	Pten	Raf1	Rb1	S100a4	Serpinb2	Serpine1	Sykb	Tek	Tert
G	Tgfb1	Tgfbr1	Thbs1	Timp1	Tnf	Tnfrsf10b	Tnfrsf1a	Trp53	Twist1	Vegfa	Vegfb	Vegfc

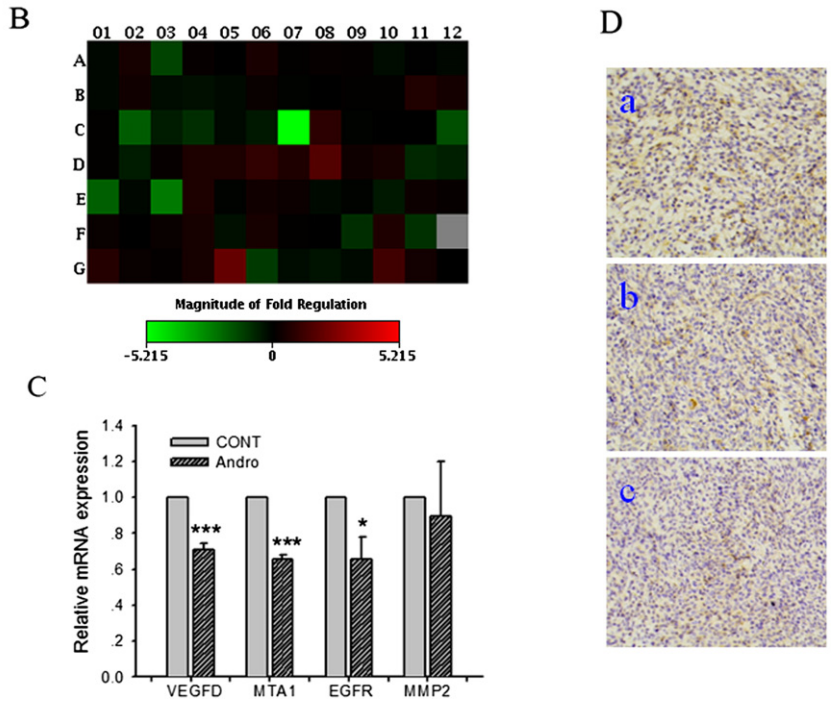

Fig. 2. Andro decreases VEGFD expression in tumor *in vivo*. **(A)** The expression profiles of 84 genes included in the Cancer PathwayFinder PCR array in control and Andro-treated mice. The layout of the genes included in the Cancer PathwayFinder PCR array. (**B**) Heat map of the variations in the expression of 84 genes between control and Andro-treated mice are shown as a fold increase or decrease. (**C**) Real-time PCR is used to detect VEGFD, MTA1, EGFR and MMP2 mRNA expression in tumor *in vivo*. Data are expressed as means ± SEM (n = 6). $^{*}P < 0.05$, $^{***}P < 0.001$ versus control. **(D)** Representative pictures of tumor immunohistochemical staining of VEGFD. a, Control, b, Andro (5 mg/kg), c, Andro (10 mg/kg) (Original magnification × 200).

in Table 1. From the results, we can see that the alternation of four genes is over three-folds between control and Andro-treated group; including VEGFD, metastasis associated 1(MTA1), matrix metallopeptidase 2 (MMP2), and epidermal growth factor receptor (EGFR). Of which, the alternation of VEGFD was the highest.

Next, we used real-time PCR assay to further confirm the alternation of those above four genes found in Cancer PathwayFinder RT^2 Profiler™ PCR array. The results showed that the mRNA expression of VEGFD, MTA1, and EGFR was decreased in tumor tissues of Andro (10 mg/kg)-treated group ($P < 0.05$, $P < 0.001$) (Fig. 2C). In addition, the results of immunohistochemical analysis of VEGFD in tumor tissues further confirmed the decreased expression of VEGFD in Andro-treated group (Fig. 2D).

3.3. Andro decreased VEGFD expression in hepatoma cancer cells

As shown in Fig. 3A, Andro (50 μM) decreased mRNA expression of VEGFD in hepatoma Hep3B and HepG2 cells ($P < 0.05$). The results of Western-blot demonstrated that Andro (50 μM) decreased the protein expression of VEGFD in a time-dependent manner in Hep3B cells (Fig. 3B). The results of calculating the density of protein bands further evidenced the decreased expression of VEGFD induced by Andro (50 μM) in Hep3B cells ($P < 0.05$, $P < 0.01$) (Fig. 3C). In addition, the ELISA results showed that Andro (25 and 50 μM) decreased VEGFD amount in Hep3B cell supernatants ($P < 0.05$, $P < 0.05$) (Fig. 3D).

3.4. Andro decreased cFos expression in hepatoma cancer cells

Next, we observed the mRNA expression of cFos, and the results showed that Andro (50 μM) had no effect on cFos mRNA expression (Fig. 4A). Further results showed that Andro (50 μM) decreased cFos protein expression in a time-dependent manner in Hep3B cells (Fig. 4B and C). In addition, Andro (50 μM) also decreased the translocation of cFos from cytoplasm to nucleus in Hep3B cells (Fig. 4D and E). As cFos is an important member of transcription factor activator protein-1 (AP-1). Next, the transcriptional activity of AP-1 was determined. The results showed that Andro (50 μM) decreased the transcriptional activity of AP-1 after incubated with cells for 12 h and 24 h (Fig. 4F).

Table 1
The genes that expressed differently between Andrographolide (ANDRO) and control (CONT) (fold change > 3.0).

Symbol	Accession no.	Description	ANDRO/CONT	Pathway/function
FIGF (VEGFD)	NM_010216	C-fos induced growth factor	0.14	Angiogenesis
MTA1	NM_054081	Metastasis associated 1	0.26	Invasion and metastasis
MMP2	NM_008610	Matrix metallopeptidase 2	0.30	Invasion and metastasis
EGFR	NM_007912	Epidermal growth factor receptor	0.31	Angiogenesis

3.5. Andro induced cFos protein degradation in Hep3B cells

MG132 is a specific inhibitor of proteasome and can prevent protein degradation mediated by ubiquitin/proteasome. If the decreased expression of cFos is due to the degradation via ubiquitin/proteasome pathway, inhibiting the activity of proteasome shall accumulate polyubiquitinated cFos. The results showed that Andro (25 μM and 50 μM) induced polyubiquitination of cFos protein in Hep3B cells (Fig. 5A) after cells were pretreated with MG132 (20 μM) for 2 h, which indicates the presence of ubiquitin/proteasome-mediated cFos protein degradation. Furthermore, the application of MG132 reversed the decreased expression of cFos protein after cells were incubated with Andro (50 μM) for 24 h ($P < 0.05$) (Fig. 5B and C). In addition, the decreased mRNA and protein expressions of VEGFD induced by Andro in Hep3B cells were both reversed by MG132 (20 μM) after cells were incubated with Andro (50 μM) for 24 h ($P < 0.05$, $P < 0.01$) (Fig. 5D–F).

3.6. SP600125 reversed Andro-induced the deceased expression of cFos and VEGFD

Previous study has already shown the activation of JNK induced by Andro in Hep3B cells; and further results demonstrated the important roles of the crosstalk between JNK activation and glutathione homeostasis in Andro-induced hepatoma tumor growth inhibition [9,10]. Next, whether JNK has some effect on the Andro-induced decreased expression of VEGFD or cFos is observed. As shown in Fig. 6A and B, Andro (50 μM) decreased cFos protein expression in Hep3B cells after being incubated with cells for 24 h ($P < 0.01$). Whereas, JNK inhibitor SP600125 (20 μM) reversed this decreased expression of cFos protein induced by Andro in Hep3B cells ($P < 0.05$). In addition, SP600125 also reversed the decreased mRNA and protein expression of VEGFD induced by Andro in Hep3B cells after cells were incubated with Andro (50 μM) for 24 h ($P < 0.05$) (Fig. 6C–E)

4. Discussion

Hepatocellular carcinoma (HCC) is one of the most common solid tumors worldwide, and it is the 2nd most frequent cause of cancer-related death in men and the 6th in women [21]. According to the statistical analysis in 2012, HCC is the third most fatal cancer in the world [22]. At the early stage of HCC, the most effective therapeutic strategy is surgical resection; however it suffers from a high recurrence rate exceeding 50% in 2 years [23,24]. Another choice is liver transplantation [23], but it is hampered by the lack of organ availability. Since 2008, systemic therapy with sorafenib, which is a multikinase inhibitor targeting angiogenesis, has become the standard care for un-resectable or advanced-stage HCC, but its improvement on overall survival is not much surprising

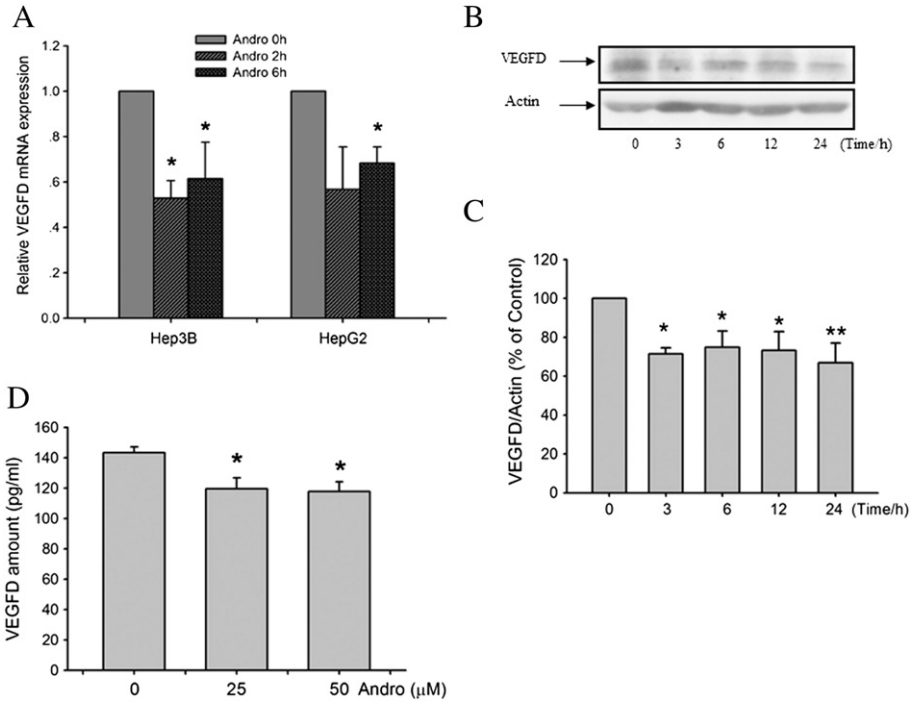

Fig. 3. Andro decreases VEGFD expression in hepatoma cells. (A) Hep3B or HepG2 cells are incubated with Andro (50 μM) for the indicated time. The mRNA expression of VEGFD is detected by real-time PCR. Data are expressed as means ± SEM (n = 4). $^{*}P < 0.05$ versus control. **(B)** Hep3B cells are incubated with Andro (50 μM) for the indicated time. VEGFD expression is detected by immunoblotting using specific antibody, and β-actin is used as loading control. Results represent three repeated experiments. **(C)** The quantitative densitometric analysis of VEGFD protein. Data are expressed as means ± SEM (n = 3). $^{*}P < 0.05$, $^{**}P < 0.01$ versus control. (D) Hep3B cells were incubated with Andro (25 and 50 μM) for 24 h, and the release of VEGFD into the supernatant was determined by ELISA. Data are expressed as means ± SEM (n = 4). $^{*}P < 0.05$ versus control.

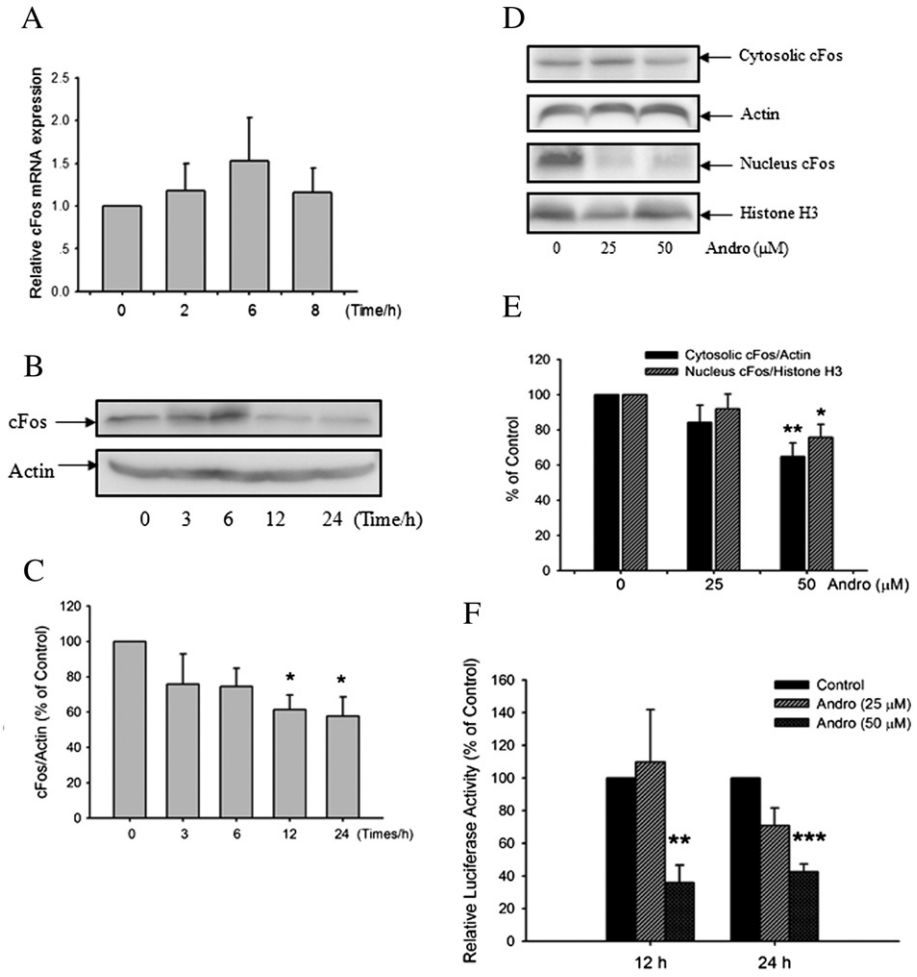

Fig. 4. Andro decreases cFos expression in hepatoma cells. Hep3B cells are incubated with Andro (50 μM) for the indicated time. (**A**) The mRNA expression of cFos. Data are expressed as means ± SEM (n = 4). (**B**) cFos expression is detected by immunoblotting using specific antibody, and β-actin is used as loading control. Results represent at least three repeated experiments. (**C**) The quantitative densitometric analysis of cFos protein. Data are expressed as means ± SEM (n = 4). $^{*}P < 0.05$ versus control. (**D**) The translocation of cFos from cytoplasm into nucleus is detected by immunoblotting using specific antibody. β-actin and histone H3 are used as loading control for cytoplasm or nucleus, respectively. Results represent at least three repeated experiments. (**E**) The quantitative densitometric analysis of cFos protein. Data are expressed as means ± SEM (n = 4). $^{*}P < 0.05$, $^{**}P < 0.01$ versus control. (**F**) Hep3B cells were transfected with pGL4.32 (*luc*2P/AP-1/Hygo). At 24 h after transfection, cells were treated with or without Andro for 12 h and 24 h. Luciferase activity was measured using the Duan-Glo® Luciferase Assay System. Results were expressed as the percentage (%) of normalized luciferase activities between Andro-treated and Andro-untreated cells. Data are expressed means ± SEM (n = 6). $^{**}P < 0.01$, $^{***}P < 0.001$ versus control.

[25]. Therefore, the development of more effective drug for HCC treatment is urgently needed.

Natural product Andro is the main compound in *Andrographis paniculata*, our previous studies and results of other groups showed that Andro was reported to have anti-tumor effect on hepatoma cancer *in vivo* and *in vitro* [3,8–11,26]. In the present study, Cancer PathwayFinder RT^2 Profiler™ PCR array was used to find out the potentially involved signals in Andro-induced inhibition on hepatoma tumor growth. The results demonstrated that the mRNA expression of VEGFD, MTA1, EGFR, and MMP2 was obviously decreased in tumors with Andro treatment. Further real-time PCR result confirmed that the mRNA expression of VEGFD, MTA1 and EGFR was decreased in Andro-treated group. VEGFD is an important pro-angiogenic factor, and the decreased expression of VEGFD mRNA is the highest of all those changed genes in Andro-treated group. In addition, after staining with VEGFD antibody in tumor tissue, we can see that the expression of VEGFD is obviously decreased in Andro-treated group. Further results in hepatoma Hep3B and HepG2 cells, we also observed the decreased expression of VEGD. VEGFD was isolated as a cFos oncogene-inducible mitogen [27], and it is primarily found in skeletal muscle, heart, lung, and intestine [28]. More and more evidences proved that high VEGFD expression was related with tumor growth and metastasis [16–19,29–31]. In addition, there are some reports about the promotion of VEGFD on the tumor growth and metastasis of hepatocellular carcinoma [32,33]. Thus, the decreased expression of VEGFD will contribute to the inhibition of Andro on hepatoma cancer growth.

As VEGFD is a cFos-inducible gene, so we observed the expression of cFos in hepatoma cancer cells. Our results showed that Andro decreased cFos protein expression and its nuclear translocation. Transcriptional factor AP-1 is a heterodimeric protein composed of proteins including cFos, c-Jun, JunD, etc. [34]. Further results showed that Andro decreased the transcriptional activity of AP-1, which may be attributed to the decreased expression of cFos. However, further results showed that Andro had no effect on cFos mRNA expression. As the Andro-induced decreased expression of cFos is not due to the inhibition on its mRNA expression, we further observed the protein degradation of cFos induced by Andro in the following experiments. The results showed that Andro induced the polyubiquitination of cFos protein at the presence of MG132. In addition, MG132 reversed the decreased expression of cFos protein, and further reversed the decreased expression of VEGFD mRNA and protein induced by Andro. Our present study indicates that Andro may induce the ubiquitin/proteasome-mediated cFos protein

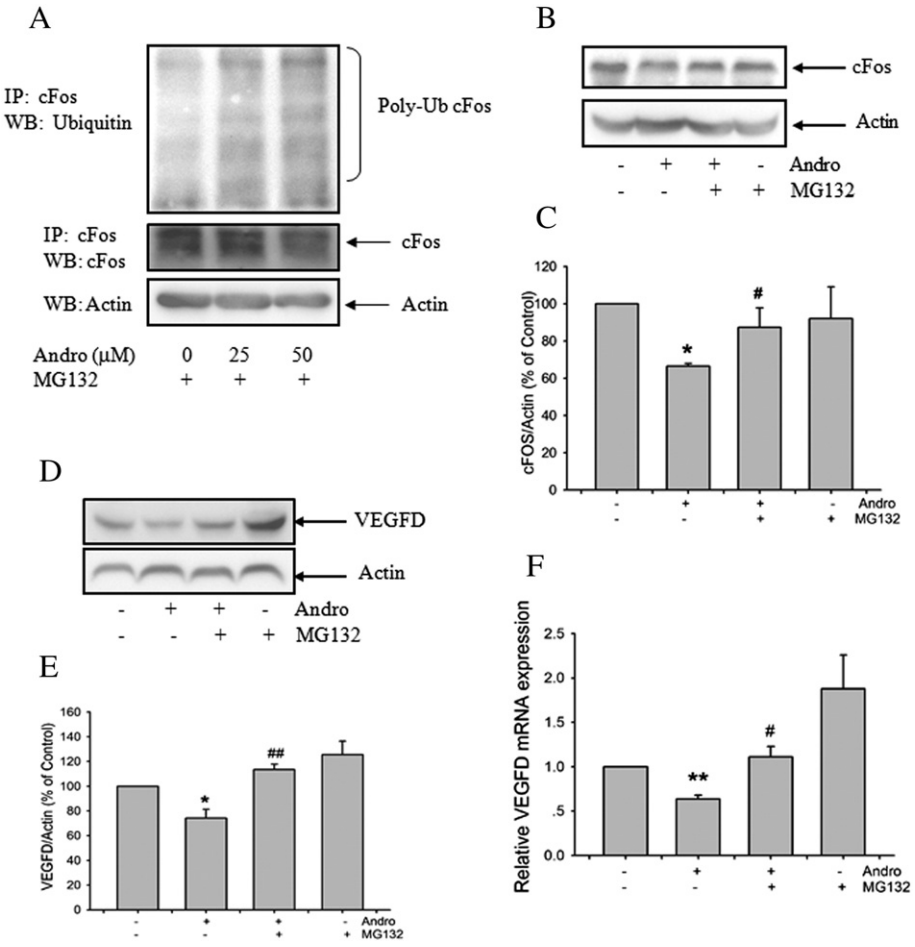

Fig. 5. Andro induces ubiquitin-dependent proteasomal degradation of cFos protein. (**A**) Hep3B cells are pretreated with MG132 (20 μM) for 2 h, and then are incubated with Andro (25 and 50 μM) for another 24 h. Cell extracts are subjected to immunoprecipitation with anti-cFos antibody and the conjugates are detected with anti-ubiquitin and anti-cFos antibodies. Each blot represents one of three independent experiments. (**B**) Hep3B cells are pretreated with MG132 (20 μM) for 2 h, and then are incubated with Andro (50 μM) for another 24 h. cFos expression is detected by immunoblotting using specific antibody, and β-actin is used as loading control. Results represent at least three repeated experiments. (**C**) The quantitative densitometric analysis of cFos protein. Data are expressed as means ± SEM (n = 4). $^{*}P < 0.05$ versus control; $^{\#}P < 0.05$ versus Andro. (**D**) Hep3B cells are pretreated with MG132 (20 μM) for 2 h, and then are incubated with Andro (50 μM) for another 24 h. VEGFD expression is detected by immunoblotting using specific antibody, and β-actin is used as loading control. Results represent at least three repeated experiments. (**E**) The quantitative densitometric analysis of VEGFD protein. Data are expressed as means ± SEM (n = 3). $^{*}P < 0.05$ versus control; $^{\#\#}P < 0.01$ versus Andro. (**F**) Hep3B cells are pretreated with MG132 (20 μM) for 2 h, and then are incubated with Andro (50 μM) for another 24 h. mRNA expression of VEGFD are analyzed. Data are expressed as means ± SEM (n = 5). $^{**}P < 0.01$ versus control; $^{\#}P < 0.05$ versus Andro.

degradation, and thus lead to the decreased expression of VEGFD in hepatoma cancer cells. There are already reports that demonstrate the ubiquitin-dependent proteasomal degradation of cFos protein [35,36]; however, the molecular mechanisms and concrete molecules involved in the degradation system of cFos protein are still not known at all. The E3 ubiquitin ligase UBR1 and a novel species of E3 ubiquitin ligase have been reported to be involved in regulating cFos protein degradation [37,38], and these two E3 ubiquitin ligases may also be involved in Andro-induced cFos protein degradation, which needs further investigation.

JNK belongs to the family of mitogen-activated protein kinase (MAPK). Our previous studies have demonstrated that Andro induced the phosphorylated activation of JNK in hepatoma cancer cells, and which plays important roles in regulating hepatoma cancer cell growth [9,10]. Next, we observed the effect of Andro-induced JNK activation on the decreased expression of cFos and VEGFD. Our results showed that JNK inhibitor SP600125 reversed Andro-induced the decreased expression of cFos and VEGFD in hepatoma cancer cells. There are already reports evidenced that other members of MAPK family such as ERK1/2 and ERK5 play important roles in regulating the transcriptional activation of cFos via stabilizing cFos protein [39–41]. Our present study indicates that JNK may promote ubiquitin-dependent proteasomal degradation of cFos protein, and thus lead to the decreased expression of cFos and its regulated downstream gene VEGFD. However, the concrete mechanism under Andro-induced cFos degradation via JNK activation needs further investigation.

5. Conclusions

Our findings demonstrate that Andro decreases VEGFD expression in hepatoma cancer cells via inducing ubiquitin-dependent proteasomal degradation of cFos protein, which will contribute to the inhibition of Andro on hepatoma tumor growth. In addition, the Andro-induced activation of JNK plays some role in regulating Andro-decreased cFos and VEGFD expression.

Supplementary data to this article can be found online at http://dx.doi.org/10.1016/j.bbagen.2015.01.005.

Transparency Document

The Transparency document associated with this article can be found, in the online version.

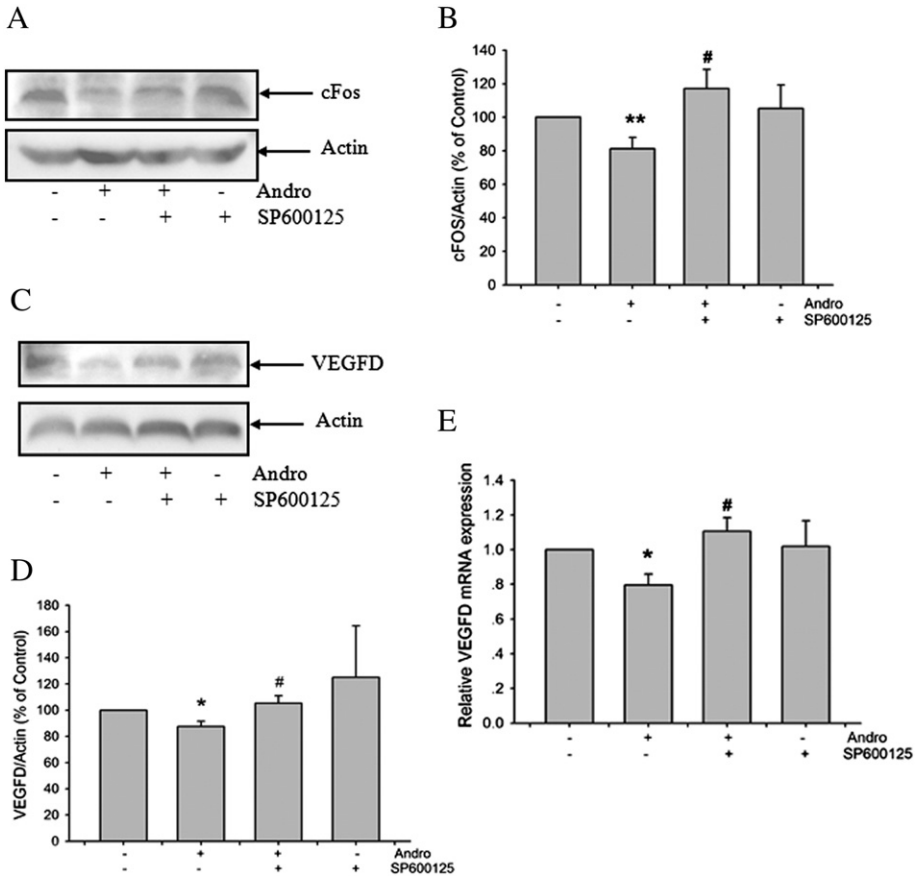

Fig. 6. Effects of SP600125 on the Andro-induced decreased expression of cFos and VEGFD. (**A**) Hep3B cells are pretreated with SP600125 (20 μM) for 15 min, and then are incubated with Andro (50 μM) for another 24 h. cFos expression is detected by immunoblotting using specific antibody, and β-actin is used as loading control. Results represent at least three repeated experiments. (**B**) The quantitative densitometric analysis of cFos protein. Data are expressed as means ± SEM (n = 5). $^{**}P < 0.01$ versus control; $^{\#}P < 0.05$ versus Andro. (**C**) Hep3B cells are pretreated with SP600125 (20 μM) for 15 min, and then are incubated with Andro (50 μM) for another 24 h. VEGFD expression is detected by immunoblotting using specific antibody, and β-actin is used as loading control. Results represent at least three repeated experiments. (**D**) The quantitative densitometric analysis of VEGFD protein. Data are expressed as means ± SEM (n = 3). $^{*}P < 0.05$ versus control; $^{\#}P < 0.05$ versus Andro. (**E**) Hep3B cells are pretreated with SP600125 (20 μM) for 15 min, and then are incubated with Andro (50 μM) for another 24 h. The mRNA expression of VEGFD is analyzed. Data are expressed as means ± SEM (n = 5). $^{*}P < 0.05$ versus control; $^{\#}P < 0.05$ versus Andro.

Acknowledgments

The authors gratefully acknowledge financial support from Training Plan of Excellent Young Medical Talents in Shanghai (XYQ2011057), and National Natural Science Foundation of China (81322053, 81173517).

References

[1] J.C. Lim, T.K. Chan, D.S. Ng, S.R. Sagineedu, J. Stanslas, W.S. Wong, Andrographolide and its analogues: versatile bioactive molecules for combating inflammation and cancer, Clin. Exp. Pharmacol. Physiol. 39 (2012) 300–310.
[2] B. Zhou, D. Zhang, X. Wu, Biological activities and corresponding SARs of andrographolide and its derivatives, Mini. Rev. Med. Chem. 13 (2013) 298–309.
[3] W. Chen, L. Feng, H. Nie, X. Zheng, Andrographolide induces autophagic cell death in human liver cancer cells through cyclophilin D-mediated mitochondrial permeability transition pore, Carcinogenesis 33 (2012) 2190–2198.
[4] Y.H. Lai, S.L. Yu, H.Y. Chen, C.C. Wang, H.W. Chen, J.J. Chen, The HLJ1-targeting drug screening identified Chinese herb andrographolide that can suppress tumor growth and invasion in non-small-cell lung cancer, Carcinogenesis 34 (2013) 1069–1080.
[5] C.Y. Chao, C.K. Lii, Y.T. Hsu, C.Y. Lu, K.L. Liu, C.C. Li, H.W. Chen, Induction of heme oxygenase-1 and inhibition of TPA-induced matrix metalloproteinase-9 expression by andrographolide in MCF-7 human breast cancer cells, Carcinogenesis 34 (2013) 1843–1851.
[6] G.Q. Bao, B.Y. Shen, C.P. Pan, Y.J. Zhang, M.M. Shi, C.H. Peng, Andrographolide causes apoptosis via inactivation of STAT3 and Akt and potentiates antitumor activity of gemcitabine in pancreatic cancer, Toxicol. Lett. 222 (2013) 23–35.
[7] S.R. Jada, C. Matthews, M.S. Saad, A.S. Hamzah, N.H. Lajis, M.F. Stevens, J. Stanslas, Benzylidene derivatives of andrographolide inhibit growth of breast and colon cancer cells in vitro by inducing G(1) arrest and apoptosis, Br. J. Pharmacol. 155 (2008) 641–654.
[8] K.K. Shen, L.L. Ji, B. Lu, C. Xu, C.Y. Gong, G. Morahan, Z.T. Wang, Andrographolide inhibits tumor angiogenesis via blocking VEGFA/VEGFR2-MAPKs signaling cascade, Chem. Biol. Interact. 218C (2014) 99–106.
[9] L.L. Ji, K.K. Shen, P. Jiang, G. Morahan, Z.T. Wang, Critical roles of cellular glutathione homeostasis and JNK activation in andrographolide-mediated apoptotic cell death in human hepatoma cells, Mol. Carcinog. 50 (2011) 580–591.
[10] L.L. Ji, T.Y. Liu, J. Liu, Y. Chen, Z.T. Wang, Andrographolide inhibits human hepatoma-derived Hep3B cell growth through the activation of c-Jun N-terminal kinase, Planta Med. 73 (2007) 1397–1401.
[11] L.L. Ji, K.K. Shen, J. Liu, Y. Chen, T.Y. Liu, Z.T. Wang, Intracellular glutathione regulates Andrographolide-induced cytotoxicity on hepatoma Hep3B cells, Redox Rep. 14 (2009) 176–184.
[12] J. Folkman, Y. Shing, Angiogenesis, J. Biol. Chem. 267 (1992) 10931–10934.
[13] F. Bahram, L. Classon-Welsh, VEGF-mediated signal transduction in lymphatic endothelial cells, Pathophysiology 17 (2010) 253–261.
[14] L. Marconcini, S. Marchio, L. Morbidelli, E. Cartocci, A. Albini, M. Ziche, F. Bussolino, S. Oliviero, c-fos-induced growth factor/vascular endothelial growth factor D induces angiogenesis in vivo and in vitro, Proc. Natl. Acad. Sci. U. S. A. 96 (1999) 9671–9676.
[15] M.G. Achen, M. Jeltsch, E. Kukk, T. Makinen, A. Vitali, A.F. Wilks, K. Alitalo, S.S. Stacker, Vascular endothelial growth factor D (VEGF-D) is a ligand for the tyrosine kinases VEGF receptor 2 (Flk) and VEGF receptor 3 (Flt4), Proc. Natl. Acad. Sci. U. S. A. 95 (1998) 548–553.
[16] S.A. Stacker, C. Caesar, M.E. Baldwin, G.E. Thornton, R.A. Williams, R. Prevo, D.G. Jackson, S. Nishikawa, H. Kubo, M.G. Achen, VEGF-D promotes the metastatic spread of tumor cells via the lymphatics, Nat. Med. 7 (2001) 186–191.
[17] J.H. Choi, Y.H. Oh, Y.W. Park, H.K. Baik, Y.Y. Lee, I.S. Kim, Correlation of vascular endothelial growth factor-D expression and VEGFR3-positive vessel density with lymph node metastasis in gastric carcinoma, J. Korean Med. Sci. 23 (2008) 592–597.
[18] G.G. Van den Eynden, I. Van der Auwera, S.J. Van Laere, X.B. Trinh, C.G. Colpaert, P. van Dam, L.Y. Dirix, P.B. Vermeulen, E.A. Van Marck, Comparison of molecular determinants of angiogenesis and lymphangiogenesis in lymph node metastases and in primary tumours of patients with breast cancer, J. Pathol. 213 (2007) 56–64.
[19] J. Wang, Y. Guo, B.C. Wang, J.W. Bi, K.N. Li, X.J. Liang, H. Chu, H. Jiang, Lymphatic microvessel density and vascular endothelial growth factor-C and -D as prognostic factors in breast cancer: a systematic review and meta-analysis of the literature, Mol. Biol. Rep. 39 (2012) 11153–111565.
[20] T. Karpanen, K. Alitalo, Lymphatic vessels as targets of tumor therapy, J. Exp. Med. 194 (2001) F37–F42.

[21] J. Ferlay, H.R. Shin, F. Bray, D. Forman, C. Mathers, D.M. Parkin, Estimates of worldwide burden of cancer in 2008: globocan 2008, Int. J. Cancer 127 (2010) 2893–2917.
[22] A. Jemal, F. Bray, M.M. Center, J. Ferlay, E. Ward, D. Forman, Global cancer statistics, CA Cancer J. Clin. 61 (2011) 69–90.
[23] A. Flores, J.A. Marrero, Emerging trends in hepatocellular carcinoma: focus on diagnosis and therapeutics, Clin. Med. Insights Oncol. 8 (2014) 71–76.
[24] C. Cha, Y. Fong, W.R. Jarnagin, L.H. Blumgart, R.P. DeMatteo, Predictors and patterns of recurrence after resection of hepatocellular carcinoma, J. Am. Coll. Surg. 197 (2003) 753–758.
[25] M. Peck-Radosavljevic, Drug therapy for advanced-stage liver cancer, Liver Cancer 3 (2014) 125–131.
[26] L. Yang, D. Wu, K. Luo, S. Wu, P. Wu, Andrographolide enhances 5-fluorouracil-induced apoptosis via caspase-8-dependent mitochondrial pathway involving p53 participation in hepatocellular carcinoma (SMMC-7721) cells, Cancer Lett. 276 (2009) 180–188.
[27] M. Orlandini, L. Marconcini, R. Ferruzzi, S. Oliviero, Identification of a c-fos-induced gene that is related to the platelet-derived growth factor/vascular endothelial growth factor family, Proc. Natl. Acad. Sci. U. S. A. 93 (1996) 11675–11680.
[28] Y. Yamada, J. Nezu, M. Shimane, Y. Hirata, Molecular cloning of a novel vascular endothelial growth factor, VEGF-D, Genomics 42 (1997) 483–488.
[29] T. Yu, Z. Wang, K. Liu, Y. Wu, J. Fan, J. Chen, C. Li, G. Zhu, L. Li, High interstitial fluid pressure promotes tumor progression through inducing lymphatic metastasis-related protein expressions in oral squamous cell carcinoma, Clin. Transl. Oncol. 16 (2014) 539–547.
[30] Y.C. Zhao, X.J. Ni, Y. Li, M. Dai, Z.X. Yuan, Y.Y. Zhu, C.Y. Luo, Peritumoral lymphangiogenesis induced by vascular endothelial growth factor C and D promotes lymph node metastasis in breast cancer patients, World J. Surg. Oncol. 10 (2012) 165.
[31] F. Bolat, D. Gumurdulu, S. Erkanli, F. Kayaselcuk, H. Zeren, M. Ali Vardar, E. Kuscu, Maspin overexpression correlates with increased expression of vascular endothelial growth factors A, C, and D in human ovarian carcinoma, Pathol. Res. Pract. 204 (2008) 379–387.
[32] J. Deng, H. Liang, D. Sun, Y. Pan, B. Wang, Y. Guo, Vascular endothelial growth factor – D is correlated with hepatic metastasis from gastri cancer after radical gastrectomy, Surgey 146 (2009) 896–905.
[33] A. Thelen, A. Scholz, C. Benckert, Z. von Marschall, M. Schroder, B. Wiedenmann, P. Neuhaus, S. Rosewicz, S. Jonas, VEGF-D promotes tumor growth and lymphatic spread in a mouse model of hepatocellular carcinoma, Int. J. Cancer 122 (2008) 2471–2481.
[34] J. Hess, P. Angel, M. Schorpp-Kistner, AP-1 subunits: quarrel and harmony among siblings, J. Cell Sci. 117 (2004) 5965–5973.
[35] J. Basbous, I. Jariel-Encontre, T. Gomard, G. Bossis, M. Piechaczyk, Ubiquitin-independent-versus ubiquitin-dependent proteasomal degradation of the c-Fos and Fra-1 transcription factors: is there a unique answer? Biochimie 90 (2008) 296–305.
[36] T. Gomard, I. Jariel-Encontre, J. Basbous, G. Bossis, G. Mocquet-Torcy, Fos family protein degradation by the proteasome, Biochem. Soc. Trans. 36 (2008) 858–863.
[37] I. Stancovski, H. Gonen, A. Orian, A.L. Schwartz, A. Ciechanover, Degradation of the Proto-Oncogene product c-Fos by the Ubiquitin proteolytic system in vivo and in vitro: identification and characterization of the conjugating enzymes, Mol. Cell. Biol. 15 (1995) 7106–7116.
[38] T. Sasaki, H. Kojima, R. Kishimoto, A. Ikeda, H. Kunimoto, K. Nakajima, Spatiotemporal regulation of c-Fos by ERK5 and the E3 ubiquitin ligase UBR1, and its biological role, Mol. Cell 24 (2006) 63–75.
[39] K. Terasawa, K. Okazaki, E. Nishida, Regulation of c-Fos and Fra-1 by the MEK5-ERK5 pathway, Genes Cells 8 (2003) 263–273.
[40] R.H. Chen, P.C. Juo, T. Curran, J. Blenis, Phosphorylation of c-Fos at the C-terminus enhances its transforming activity, Oncogene 12 (1996) 1493e1502.
[41] P. Monje, M.J. Marinissen, J.S. Gutkind, Phosphorylation of the carboxyl-terminal transactivation domain of c-Fos by extracellular signal-regulated kinase mediates the transcriptional activation of AP-1 and cellular transformation induced by platelet-derived growth factor, Mol. Cell. Biol. 23 (2003) 7030e7043.